LASER INTERFEROMETER GRAVITATIONAL WAVE OBSERVATORY
- LIGO -
CALIFORNIA INSTITUTE OF TECHNOLOGY
MASSACHUSETTS INSTITUTE OF TECHNOLOGY

Publication **LIGO-T010108-00 – D** 9/28/01

Analysis of Lightning Events

Janice Hester

Distribution of this draft:

all

This is a technical note of the LIGO Project.
(SURF Report)

LIGO Hanford Observatory
P.O. Box 1970 S9-02
Richland, WA 99352
Phone (509) 372-8106
FAX (509) 372-8137
E-mail: info@ligo.caltech.edu

LIGO Livingston Observatory
19100 LIGO Lane
Livingston, LA 70754
Phone (504) 686-3100
FAX (504) 686-7189
E-mail: info@ligo.caltech.edu

California Institute of Technology
LIGO Project - MS 51-33
Pasadena CA 91125
Phone (626) 395-2129
Fax (626) 304-9834
E-mail: info@ligo.caltech.edu

Massachusetts Institute of Technology
LIGO Project - MS NW17-161
Cambridge, MA 01239
Phone (617) 253-4824
Fax (617) 253-7014
E-mail: info@ligo.mit.edu

WWW: http://www.ligo.caltech.edu/

Abstract

The Laser Interferometer Gravitational-wave Observatory (LIGO) is currently building three long baseline interferometers at two sites with the goal of detecting gravitational waves from astrophysical objects. Electromagnetic radiation caused by lighting may generate coincidence events which mimic real burst events. The goal of this project is to determine both how lightning strikes of differing peak currents and distances are detected by magnetometers installed at both sites and how this information can be used to veto coincidence events. The magnetometer data was scanned for spikes associated with known events, and the relationships between signal strength, distance, and peak current examined. A "glitch" finder was then developed to search for impulses in the 60 Hz contaminated magnetometer signal. Events flagged as possible lightning strikes during LIGO's fourth engineering run are compared to a data set obtained from Global Atmospherics Inc. cataloging all cloud-to-ground lightning strikes for the run.

Introduction

Motivation/LIGO

The Laser Interferometer Gravitational-wave Observatory (LIGO) is currently developing three long baseline interferometers for use in the detection of gravitational waves. LIGO Hanford Observatory (LHO) contains two of the three interferometers. The third resides in LIGO Livingston Observatory (LLO).

General Relativity predicts that changing mass distributions create traveling ripples in space-time, termed gravitational waves. The nature of these waves is such that one traveling perpendicular to a ring of mass will cause the ring to oscillate between stretching along the x-axis and stretching along the y-axis. A LIGO type interferometer hopes to detect this distortion as a differential change in the lengths of two perpendicular interferometer arms. Several classes of astronomical objects are suspected to create gravitational waves with enough strength to be detected on the Earth. Among them are compact binary stars, super massive black holes, supernovae, and inspiralling massive objects. The capability to detect gravitational waves would enhance the understanding of such objects.[1]

To ensure that an interferometer signal is the result of a passing gravitational wave, all noise sources must be eliminated. Due to the high volume of electronic systems, electromagnetic radiation has the potential to create an event at one of the detectors. One purpose of three interferometers is to guard against false events. Were an event to be detected on one, but not all, of the interferometers, it would be discarded as local noise. However, electromagnetic radiation

travels at the speed of light, as do gravitational waves, and signals from lightning are known to travel many times the 3000 km between the two LIGO sites. Therefore EM radiation caused by lightning has the potential to affect both sites and may generate coincidence events mimicking real burst events.

Lightning

A lightning event is composed of either one or several cloud-to-ground, intracloud, or cloud-to-cloud strikes. In a study done near NASA Kennedy Space Center, Florida, cloud-to-ground strikes made up 30-40% of the observed lightning strikes while over half were intracloud. The ratio of intracloud to cloud-to-ground lightning varies with location, in general decreasing with distance from the equator. There are two general classes of strikes, those that carry negative charge and those that carry positive charge. Roughly 90% of all cloud-to-ground strikes are negative strikes. During summer thunderstorms, the fraction of positive discharges increases with increasing latitude. Louisiana sees 60-80 thunderstorm days in a year while south central Washington sees 5-20, where a thunderstorm day is defines for a given location as a day on which thunder can be heard.[2, 3]

A lightning strike begins with a leader, the initial plasma channel that grows between the cloud and the ground. A step-wise leader grows in short bursts, which vary in length from 10 to 200m, with breaks, 30-90 μs, between steps. This is in opposition to a continuous leader that grows continuously from cloud to ground. Once a strike hits ground a return strike is initiated that brings neutralizing charge up into the cloud. It is at this stage that peak currents are seen. A lingering current can remain in the plasma channel for a fraction of a second after a strike. Any secondary strikes follow the path of the first leader and develop continuously. Negative lightning events usually originate low in the cloud, propagate towards the ground via step-wise leaders, and can be composed of several strikes. Positive lightning events originate higher in the thundercloud, tend to have a continuously propagating leader, and are typically composed of only one strike.[4]

The electromagnetic field produced by lightning has three components, electrostatic, magnetostatic, and electromagnetic radiation. During a return stroke, a charged leader travels back up towards the cloud both acting to alter the charge structure of the channel and serving as a current wave front. The conducting earth creates a changing positive mirror charge. This gives rise to an electric dipole and a corresponding electric field. Variations in this dipole moment give rise to electromagnetic waves. A magnetic field is produced that is proportional to the current in the channel and the channel's length. The electrostatic component varies with distance as r^{-3}, the

magnetostatic as r^{-2}, and the radiative as r^{-1}. In the near region, r less than 15-20km, the electric field dominates. Beyond this the field is dominated by the electromagnetic radiation component.[4] The strength of the electromagnetic field produced is proportional to the change in the current, *di/dt,* during the return stroke. There is evidence to the effect that both large and small return stroke currents have roughly the same field rise times. Given this strokes with larger peak currents will have larger values of *di/dt*.[2]

The strongest field strengths are seen within 1 km from the strike. At this point, the static electric field is the greatest contributor to the field. The electric field reaches typical values of 0.5-1.0 kV/m for the first return stroke. This varies with current and has a standard deviation as high as 35-70%. The magnetic induction here can be as high as 10 μT, a strength that is comparable to the radiation component of the field. At 100 km the static components are almost completely damped. Here, electric fields are on the order of 1-10 V/m and the magnetic field gives H values of 0.001 to 0.01 A/m.[4]

Lightning Detection

A lightning strike is an impulsive event. By impulsive it is meant that it is brief in time and therefore broad in frequency. The signal from a lightning strike is strongest near 5 kHz and decreases with both increasing and decreasing frequency.[3] Those who listen to natural radio classify lightning signals into three categories, sferics, whistlers, and tweaks. A sferic is a brief signal that appears in a spectrogram as a tall narrow band. Tweaks have traveled some great distance, been dispersed, and appear first at high frequencies and fall quickly through the lower frequencies. A whistler has traveled an even greater distance and the frequencies have been further separated. Sferics last milliseconds, tweaks hundreds of a second, and whistlers can last up to 4 seconds. In order for whistlers to achieve this degree of dispersion, they must travel several times the circumference of Earth. They do this by becoming trapped in the Earth's magnetic field lines.[5] Therefore, it is the shorter duration sferics and tweaks that will associate closely with a particular strike event.

Materials and Methods

National Lightning Detection Network

The NLDN operates 47 gated wide-band magnetic direction finders with GPS pulse timing and 59 time of arrival sensors across the continental United States. They are stationed such that there is an 80-90% certainty that a first stroke within range with peak current equal to or greater than 5 kA will be detected. It is thought that upwards of 95% of all negative strikes reach

peak currents greater than 5 kA. Time, location, polarity, strike strength, and multiplicity are measured and recorded for all detected strikes. The reported flash time corresponds to the time of onset of the first return stroke. This time can be measured with precision down to about 5μs. Error in location is dependent on the strength of the strike and the strikes location relative to sensors. The quoted median accuracy over the continental United States is approximately 500m. Peak current values have uncertainties of 20-30%.[6]

LIGO has purchased several months of lightning data from the NLDN, including location, given as latitude and longitude, polarity, peak current in kA, multiplicity, and time to the second in GMT. Each strike was represented by a line of data in the following form.

dd/mm/yy	hh:mm:ss	latitude	longitude	peak current kA	multiplicity
Ex. 11/05/01	06:51:23	35.598	-101.169	-25.0 kA	2

This data was transformed into time in GPS seconds and distance from the magnetometer in km. The distance conversion was done assuming that the earth is a perfect sphere with a radius of 6350km. The error introduced by uncertainty in magnetometer position and by assuming a round earth is roughly .2%, or 2 m to the kilometer. This is less than the 500 m uncertainty quoted for the NLDN location for distances less than 250 km.

LIGO's Magnetometers

LIGO has two classes of magnetometers monitoring the magnetic fields surrounding the two detectors, 3-axis Barington flux gate magnetometers and a more sensitive arrangement consisting of large coil magnetometers. The focus for this paper was a Barington magnetometer in the x-end station at LLO. The x-end station is a building at the end of the 4 km interferometer arm that points in the x direction. X is defined by a right handed coordinate system in which z points perpendicular to the earth's surface. All data used for this project correspond to LIGO's fourth engineering run from May 11th to May 13th 2001.

The Barinigton magnetometer has a range of ±100 μT. The output voltage is directly proportional to the axial component of the total field until it swings to within 1V of the supply voltage. At this point the signal saturates. When the total signal is calculated from the three arms there is some error due to a lack of orthogonality between the three lines. However, this error is less than one percent. The voltage reading is transformed to ADC (analog-to-digital converter) counts when it is digitized. The Barington magnetometers have a bandwidth of 3 kHz, starting at

DC. The amplitude and phase response of the sensors is relatively flat up to 1 kHz, at which point the amplitude response begins dropping and the phase begins to lag.[7]

To investigate the relationships between magnetometer signal strength, distance, and peak current, the signal from several known strikes was found in the time series data from the Barington magnetometer

Writing and Testing of a Glitch Finder

A program was written to search the magnetometer data for signals from lightning strikes. This 'glitch finder' takes as input the time series signal from each of the three axis of the flux gate magnetometer and outputs that GPS time of possible lightning strikes.

The first step that the glitch finder takes is transforming the signal from the three axes into one time series that is the vector sum of the three signals. The time series is then cut into tenth second intervals. A pre-existing Fast Fourier Transform (FFT) class was used to compute a power sum across several thin frequency bands away from the 60 Hz power line noise. The frequency bands and the code that generates the power signal for each 0.1s are given below.

```
double pwr =
        sqrt(    fsN->Power(80 ,100)+fsN->Power(140,160)
                 +fsN->Power(205,215)+fsN->Power(265,275)
                 +fsN->Power(325,335)+fsN->Power(385,395)
                 +fsN->Power(445,455)+fsN->Power(505,515) );
```

Here fsN is the Fourier transform of the tenth second time series and Power is a member function of the FFT class that returns the power present in the given interval.

The glitch finder searches for statistically significant spikes in the power signal. To do this a running average and standard deviation are kept over the latest 2.5s and each new time step is compared to these measures before it is included in the average or standard deviation. This comparison consists of computing the number of standard deviations away from the average each new step sits. If a step is greater than 5σ, it is flagged as an event. When this occurs the average and standard deviation are not recomputed.

To limit the number of computations needed to compute the average and standard deviation at each point the following identities were used.

$$\sigma = \sqrt{\frac{\sum\left(\overline{x} - x\right)^2}{n-1}} = \sqrt{\frac{n}{n-1}\left[\overline{x}^2 - \overline{x^2}\right]}$$

$$\overline{x}_{new} = \overline{x}_{old} + \tfrac{1}{n}\left(x_{new} - x_{old}\right)$$

Over time the average x and x^2 values drift slightly. To adjust for this, both were recalculated from the full 2.5s series every 120 seconds, 1200 steps. It is also possible that for certain series this method will result in an attempt to take the square root of a negative number. To guard against this the function that calculates sigma checks the sign of σ^2 before taking the root and will return the negative value instead of the square if a negative σ^2 is found. When this is the case the averages are again recomputed from the original data array and used to compute sigma. In order to allow for these two adjustments an array containing the most recent 2.5s of signal is maintained at all steps.

After the glitch finder was written, it was run over the first two days of magnetometer data from the fourth engineering run. The number of correlations between the catalog and the glitch finder output was then counted to test the accuracy and efficiency of the code.

FFT's and Filtering

The glitch finder used a Fast Fourier Transform (FFT) in order to filter out 60 Hz and harmonics noise due to power lines. These transforms were not performed on an infinite time series but on a tenth second time series, resulting in a spreading of each signal in the frequency domain. The smaller the time step cut, the larger the spread in the frequency range. The window used to cut the time series before the transform is termed a hanning window. In the frequency domain this corresponds to a convolution with a bell-like curve that has a full width at half max of the inverse of the time step transformed. For the tenth second time step, this results in the lines from the power line noise having a full width half max of 10 Hz.

An FFT performs a Fourier transform on a discrete time series. When a discrete transform is done, the frequency range is limited by the number of samples recorded per second. This effect is quantized by the Nyquist theorem which states that for a signal sampled at N times a second, the maximum frequency that can be distinguished corresponds to N/2 Hz. If frequencies above this point exist, they will be 'aliased' into a lower frequency within range.[8] The LIGO magnetometers are sampled 2048 times a second, placing an upper limit on the frequency range of roughly 1kHz. The signal from the magnetometer is run through an analog filter to eliminate all signals above this frequency before it is sampled to prevent any aliasing.

Results

All data can be found in (tables 1- 12).

Discussion

Signal vs. Distance and Peak Current

Strikes appear as a sharp peak or trough in the time series from these magnetometers. In the frequency domain this corresponds to a raise in power across the spectrum for the time duration of the event (fig. 1). A typical signal from lightning as seen in LIGO's magnetometers has a duration of 0.005s and a magnetometer signal between 500-4000 counts.

Three types of data sets were assembled of the magnetometer signal size of several known lightning strikes from the NLDN data. The first data sets contained strikes with similar peak currents, within 5% of the mean, and differing distances, the second sets contains strikes with similar distances, also within 5% of the mean, and differing peak currents, the final set consisted of strikes of all distances and peak currents in which the relationship between magnetometer signal and i/r was examined. Within these data sets negative and positive strikes were distinguished from each other and plotted separately. This was done as positive strikes, in general, register stronger than negative strikes. The recorded strikes can be seen in (tables 1-9)

A power fit was made to each of the data sets by first linearizing the data and then performing a linear regression. Error in distance, peak-current, and magnetometer signal is assumed to be random rather than systematic. Therefore error in dependencies was simply taken as the error in the fits. Plots made for the various sets are in (figs 2-6). Each individual fit is given in (table10). For negative strikes the following dependencies were seen.

$$r^{-1.3\pm0.3}, i^{1.0\pm0.5}, \left(\frac{i}{r}\right)^{1.0\pm0.1}$$

Positive strikes showed dependencies of

$$r^{-0.92\pm0.05}, i^{1.2\pm0.2}, \left(\frac{i}{r}\right)^{1.11\pm0.09}$$

These observed dependencies justify classifying lightning strikes by their i/r values. For distances greater than 10 km the uncertainty in i/r is heavily dominated by the uncertainty in the peak current and will be a 20-30%. For distances below this the 500 m mean error in distance begins to dominate and the percent error will increase with decreasing distance.

Glitch Finder Efficiency

A sample strike as seen by the glitch finder is displayed in (fig. 7).

When the glitch finder was run over the first two days of data from the E4 run, a sigma value was recorded for each second known to contain a lightning strike along with the i/r value

for that strike. Due to a lack of time precision in the NLDN data, the maximum sigma value for the second was used. From these points a plot of the standard deviation vs. i/r was created and a linear fit made to this plot. The i/r value corresponding to 5σ as given by the fit was recorded. This gives a measure of the sensitivity of the glitch finder. Taking the maximum value for each second created some difficulty when making a fit to the data. Low values of i/r correspond to 1.5 to 2σ, thus increasing the intercept and decreasing the slope. To adjust for this, low value i/r strikes were discarded. The i/r value at which to cut was chosen by noting first that the intercept is ideally zero and second that a plot corresponding to lightning signals will have a good correlation value for a linear fit. In choosing the i/r value at which to cut the set of strikes, several plots were made with varying cutoffs and the plot with the best intercept and correlation chosen. The linear fits for σ vs. i/r plots, along with correlations and i/r values corresponding to 5σ can be seen in (table 11). Sample plots are shown in (fig 8). For negative strikes the i/r value corresponding to 5σ was –1.97 and for positive values was 0.55.

To test the efficiency of the glitch finder the catalog of strikes was cut to strikes with i/r values corresponding to greater than or equal to 5σ. The number of correlations between the catalog and the glitch finder output from the two day run was used to find the percentage of catalog strikes showing correlations and the percentage of magnetometer glitches showing correlations. Ideally, the catalog strikes will show 100% correlation while the glitches may easily show less than this due to other disturbances, including near-by intracloud lightning or spikes in the power lines. The percentage of known strikes that show correlations with the combined power sum is 60%. The i/r values used to cut the set of known strikes have a roughly 25% uncertainty in their values. Roughly half of all strikes sitting at the cutoff and a decreasing percentage of strikes above that point will not have had actual i/r values below the cut off. This may account for several the strikes that were not flagged. A large number, 96.6%, of signals that do not correspond to lighting are flagged by the glitch finder.

The above tests were also run with modified versions of the glitch finder that relied on only one of the eight frequency bands. When the σ vs. i/r plots were made those frequency bands that showed a near zero intercept and good correlation value for some i/r cutoff were selected for the efficiency run. It is possible that those frequency bands that did not show good intercept and correlation values show fluctuations that do not correspond to the 2.5s running window. The results from these runs are used to test the effectiveness of the multi-band scheme. The frequency ranges (205,215),(265,275), and (505,515) were chosen for efficiency comparisons. Relative efficiencies are found in (table 12). The average percentage of known strikes that showed

correlations was 40%, lower than that for the multi-band scheme. The average percentage of flagged magnetometer signals was 0.9%, higher than that for multiple bands.

The multiple frequency bands are used to increase the finder's sensitivity to lightning and to limit the number of non-lightning signals that are flagged. Only an impulsive event, such as lightning, will appear in a broad frequency range. The use of multiple bands does increase the finder's sensitivity to lightning. However, it does not work in discarding as many non-lightning events as it might. It is likely that the combined power sum is picking up all glitches that appear in one or a few of the bands, as opposed to limiting glitches to those that appear only in all bands.

Intersite Correlations

The distance between the two interferometer sites is 3000km. The magnetometer and glitch finder must therefore be able to detect a strike at least 1500km away. For the current sensitivity values a strike 1000km away would need to be larger than either -1970 kA or 550 kA, depending on polarity, in order to appear on the flux gates at the two sites. The largest strike seen during the engineering run was a bit over 200kA. It is therefore unlikely that the current scheme operating on the flux gates will detect coincidences. However, the coil magnetometers are several times more sensitive than the flux gates, and it is possible that an extremely strong strike could be detected on the coils at distances great enough to cause coincidences.

Conclusions

A 'glitch finder' was written which has the ability to detect ligthning strikes with i/r (peak current/distance) values either lower than –1.97 A/m or greater than 0.55 A/m with a 60% efficiency when running on a Barington magnetomter at the LIGO Loiussiana Observatory. The glitch finder also picks up a large volume of signals that are not the result of lightning events. The strength of the signal from lighting is seen to be directly proportional to i/r. Therefore, the strength of the signal that any given lightning strike is expected to produce can be be expressed in terms of i/r. This can be used to determine what strikes have to potential for detection at both interferometer sites. It is possilbe that the coil magnetometers with greater sensitivity will detect strikes at distances great enough to allow the possibility of intersite lightning detection correlations.

References

[1] D. Sigg *Gravitational Waves*. Proceedings of TASI 90 (Theoretical Advanced Study Institute in Elementary Particle Physics) 1998.

[2] M. A. Uman, E. P. Krider, *Natural and Artificially Initiated Lightning*, Science. 246, 457 (October 1989)

[3] M. A. Uman, All About Lightning (Dover Publications Inc. New York, NY. 1986)

[4] E. M. Bazelyan, Y. P. Raizer, Lightning Physics and Lightning Protection (Institute of Phyisics Publishing. Philadelphia, Pa. 2000)

[5] B. Pine, *An Introduction to Natural Radio,* image.gsfc.nasa.gov/ poetry/inspire/intro.html.

[6] K. L. Cummins, E. P. Krider, M. D. Malone, *The U.S. National Lightning Detection Network and Applications of Cloud-to-Ground Lighting Data by Electric Power Utilities*, IEEE Transactions on Electromagnetic Compatibility, V. 40 n. 4 p. 465 (November 1998)

[7] Barington MAG-03: Three Axis Magnetic Field Sensors, Operational Manual, (GMW Associates, Recv'd 1999)

[8] W. H. Press, S. A. Teukolsky, W. T. Vetterling, B. P. Flannery, Numerical Recipies in C, Second Edition (Cambridge University Press. Cambridge, NY. 1992).

Captions

Figures

1 a) Peaks in the time series corresponding to the signal from a lightning strike. This particular strike had a peak current of 131kA and was located 86 km from the LLO x-end.

b) Broadband power increase in the frequency domain for the second of the event. The current second shower a 2-3 fold increase in power between the 60 Hz lines.

2 Plot of magnetometer signal in ADC counts versus i/r in A/m for all negative, and then all positive, strikes recorded. The m and δm correspond to the power dependency of the signal on i/r as determined by a linear fit to a double log plot. Similar plots for all data subsets are found in figures 3-6.

3 Plots for subsets of negative strikes with constant distance and varying peak currents.

4 Plots for subsets of positive strikes with constant distances and varying peak currents.

5 Plots for subsets of negative strikes with constant peak currents and varying distances.

6 Plots for subsets of positive strikes with constant peak currents and varying distances.

7 Glitch finder signal for 10s of data containing a strike. This is again the 131 kA strike at 86 km from LLO's x-end.

8 The standard deviations from the average as found by the glitch finder is plotted against i/r for a set of first negative and then positive strikes.

Tables

1 All negative recorded strikes.

Col 1	i/r values for each strike
Col 2/3	peak current and distance from LLO x-end
Col 4-7	magnetometer signal measured in the individual axes
Col 8	vector sum of the magnetometer signals

2 Tables 2-5 contain subsets of the negative strikes. This particular table shows a set centered on 48 kA at varying distances from the magnetometer.

3 Negative strikes centered on 91 kA, also with varying distances.

4 Negative strikes located around 28 km with varying peak currents.

5 Negative strikes located around 25.5 km with varying peak currents.

6 All positive recorded strikes. Columns are identical to those in table 1.

7 Tables 7-9 contain subsets of the positive strikes. This table contains strikes with peak currents centered on 87 kA at varying distances.

8 Positive strikes located around 21 km with varying peak currents.

9 Positive strikes located around 87.5 km with varying peak currents.

10 Power dependency for each set of strikes on i, r, or i/r. m is the slope of the linear fit to a double log plot of the respective data sets. The combined rows give the average dependency for a given variable. For example, the value for the distance-combined is the average of the values for the set with peak currents centered on 48 kA and that centered on 91 kA.

11 Linear fits for σ vs. i/r for the glitch finder running with all eight frequency bands and running with each of the individual bands.

Col 1	frequency band/s the finder was using
Col 2	i/r value below which strikes were discarded
Col 3&4	Slope of the linear fit
Col 5&6	Intercept of the linear fit
Col 7	Correlation value for the fit
Col 8	i/r value corresponding to 5σ

Those fits with unacceptable intercept and correlation values were not used for efficiency measurements and have been struck out.

12 Measurements of the efficiency of the finder for both the eight-band glitch finder and three individual bands.

Col 1	frequency band/s the finder was using
Col 2	number of glitches found by the glitch finder
Col 3	number of strikes during the time the finder was run with i/r values above the cutoff point for each band/set of bands
Col 4	number of correlations between glitches and known strikes
Col 5	percentage of glitches that showed correlations
Col 6	percentage of known strikes that showed correlations

Figure 1 (a,b)

a)

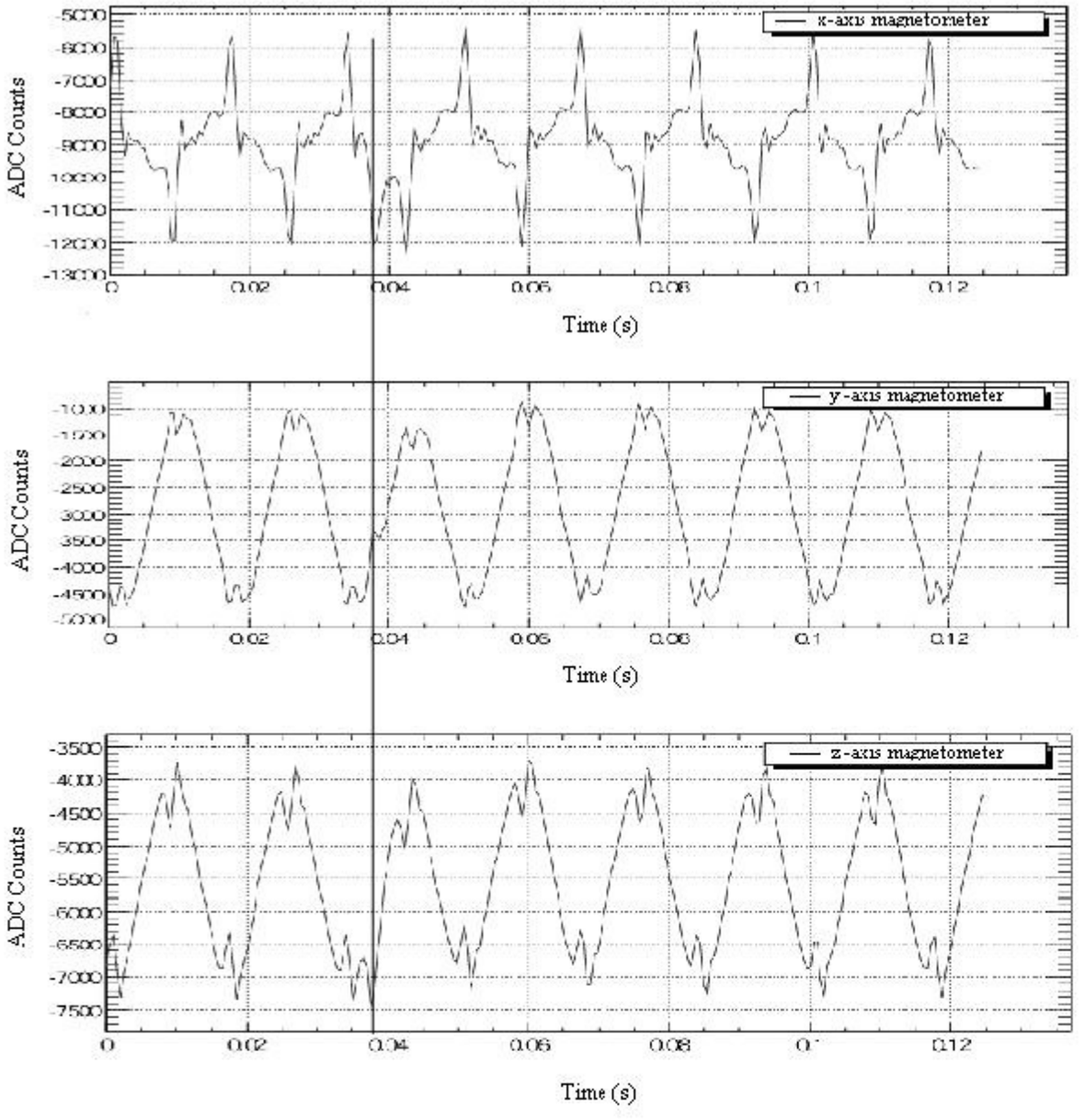

b)

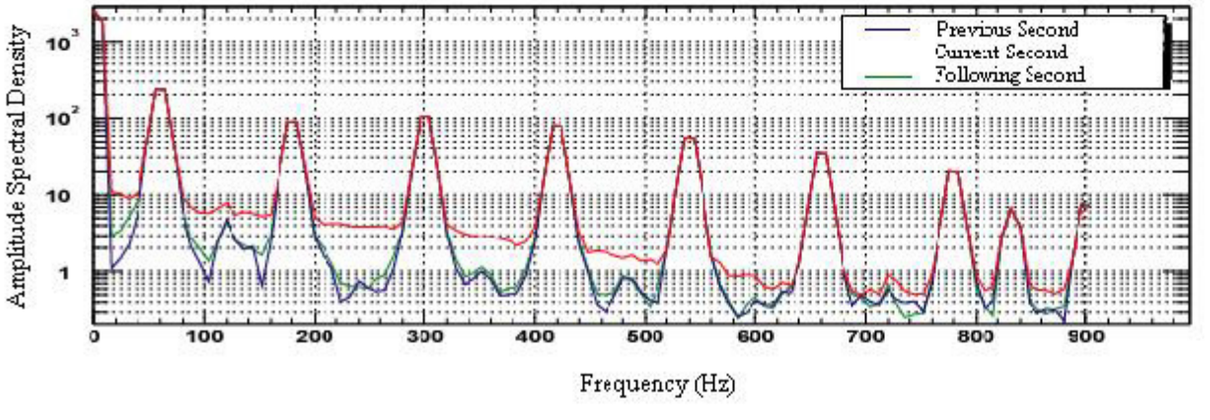

Figure 2

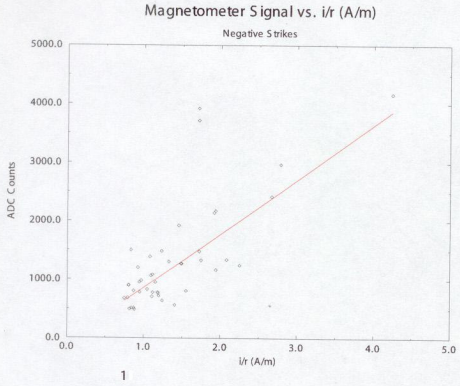

m = 1.0
δm = 0.14

1

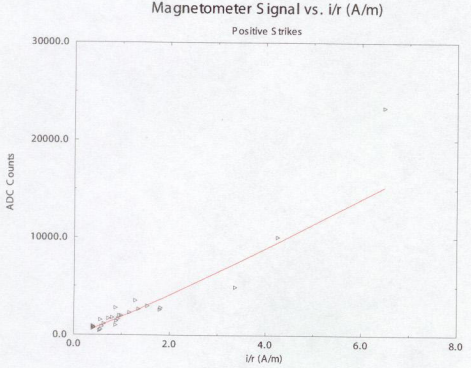

m = 1.1
δm = 0.1

Figure 3

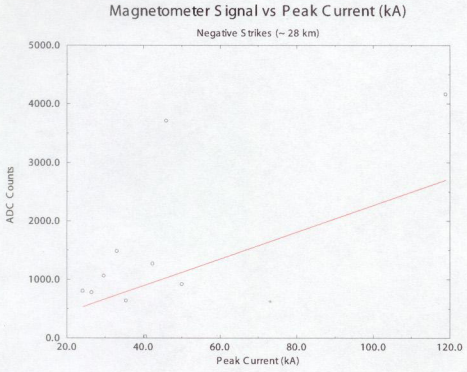

m = 1
δm = 1

1.0

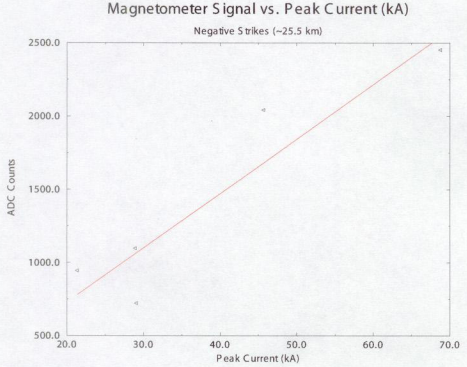

m = 1.0
δm = 0.14

Figure 4

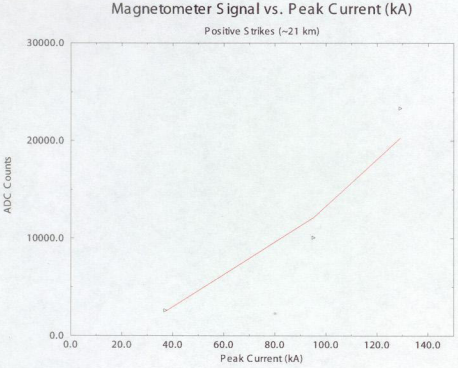

$m = 1.7$
$\delta m = 0.3$

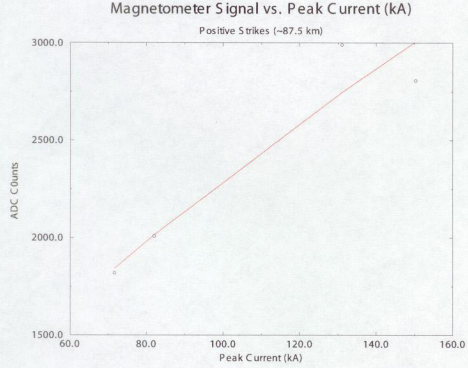

$m = 0.7$
$\delta m = 0.13$

Figure 5

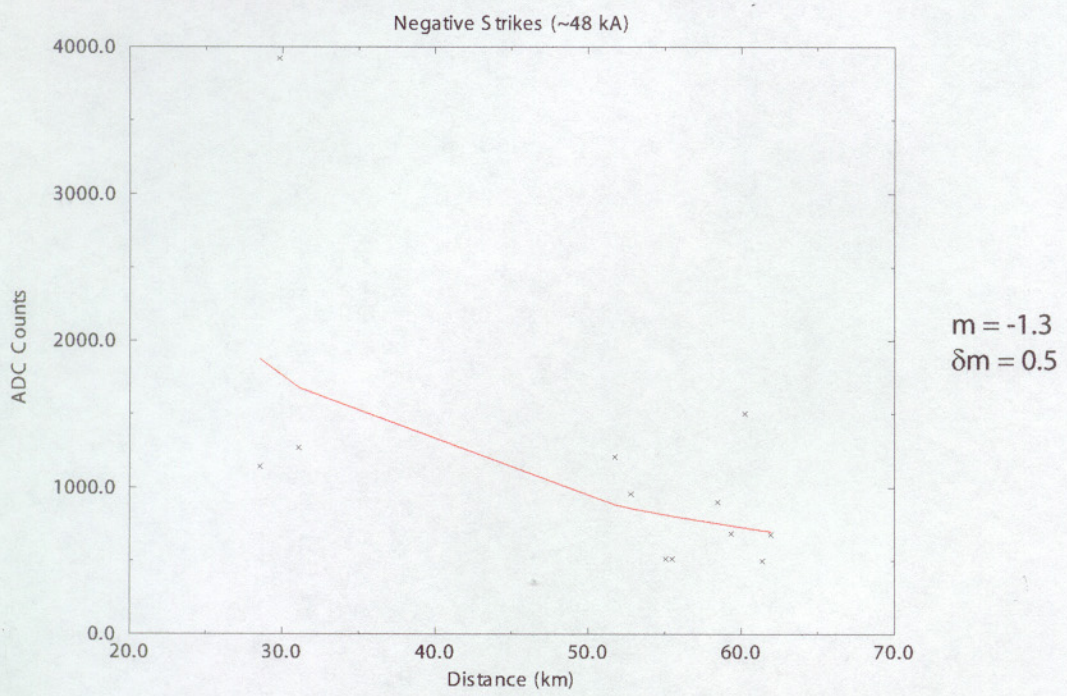

$m = -1.3$
$\delta m = 0.5$

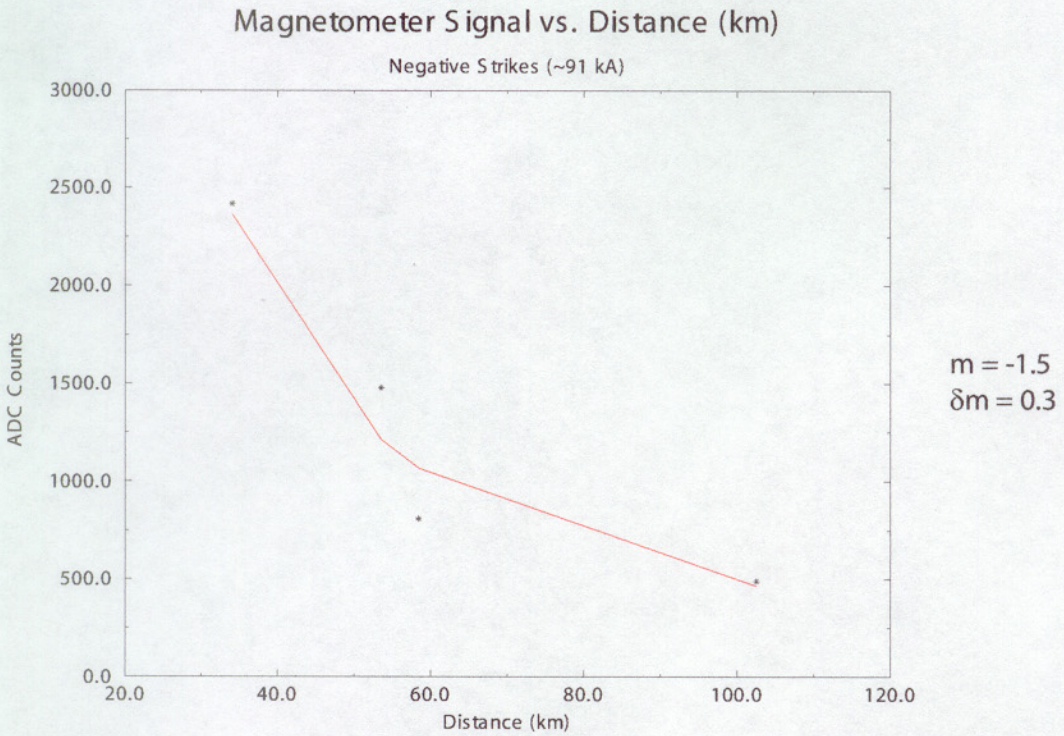

$m = -1.5$
$\delta m = 0.3$

Figure 6

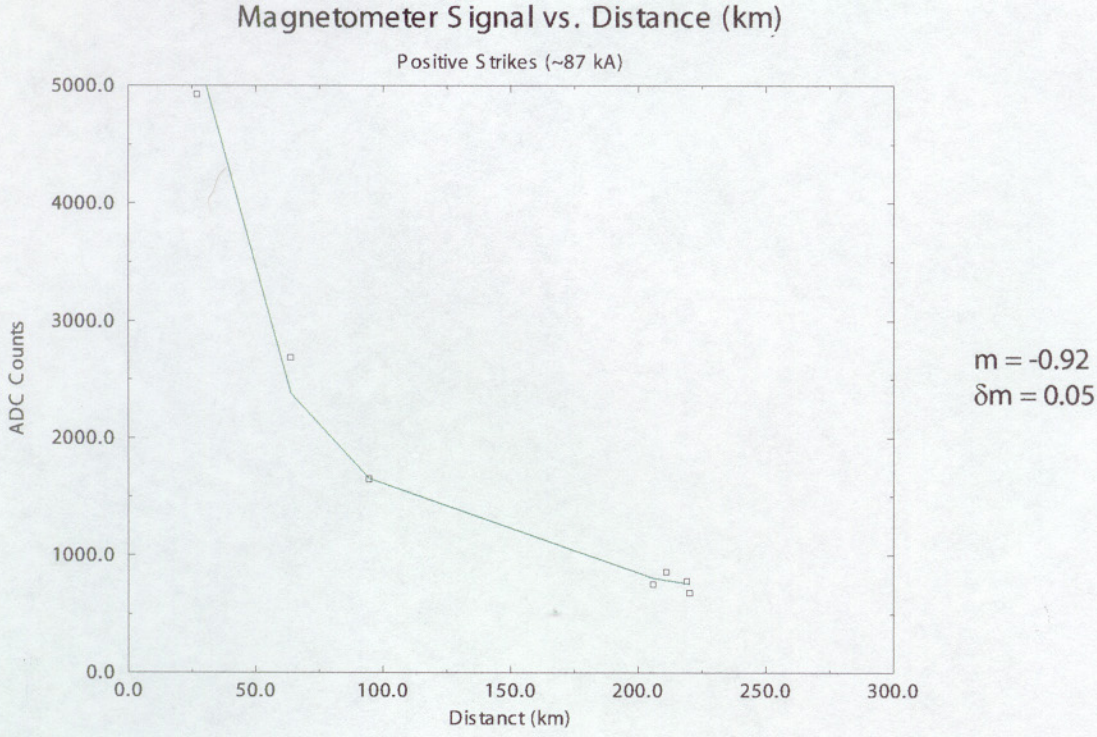

$m = -0.92$

$\delta m = 0.05$

Figure 7

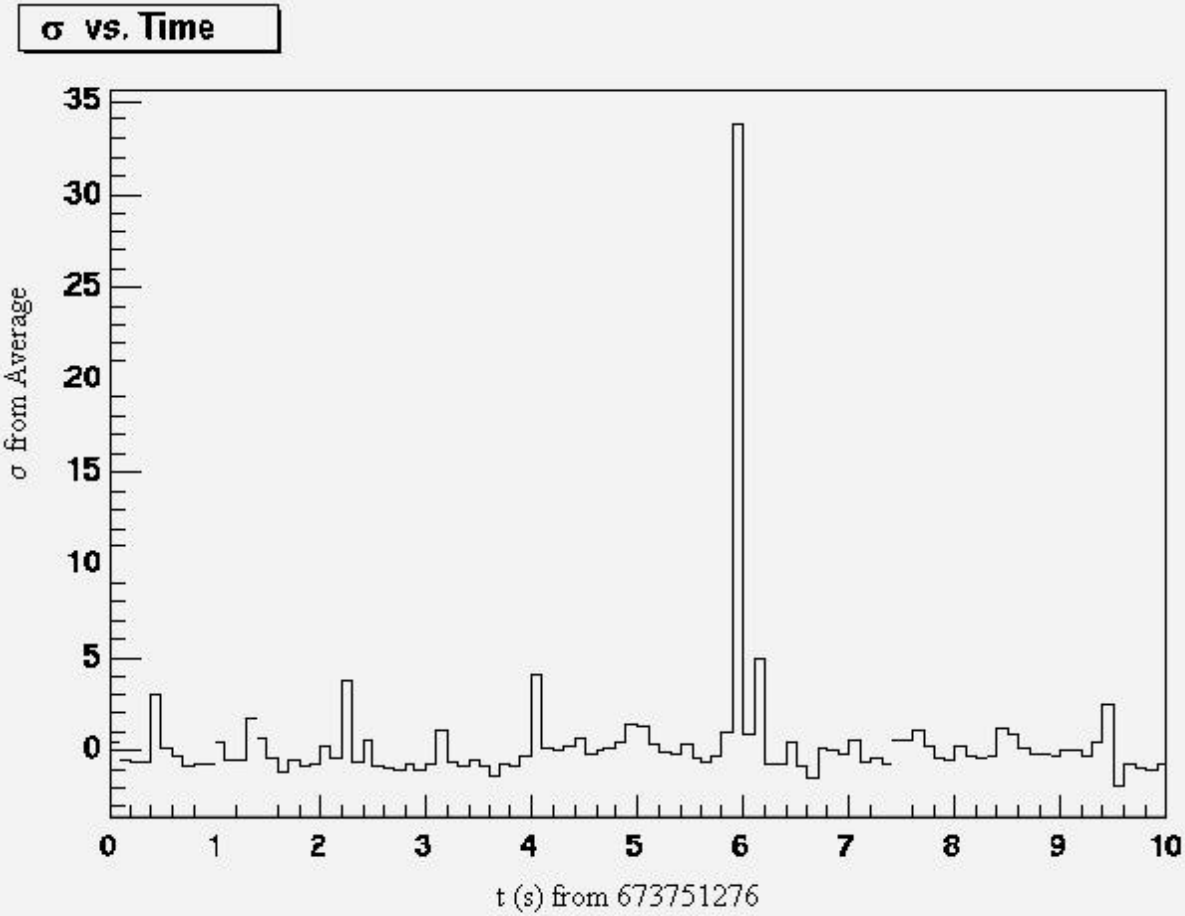
σ vs. Time
σ from Average
35
30
25
20
15
10
5
0
0
1
2
3
4
5
6
7
8
9
10
t (s) from 673751276

Figure 8

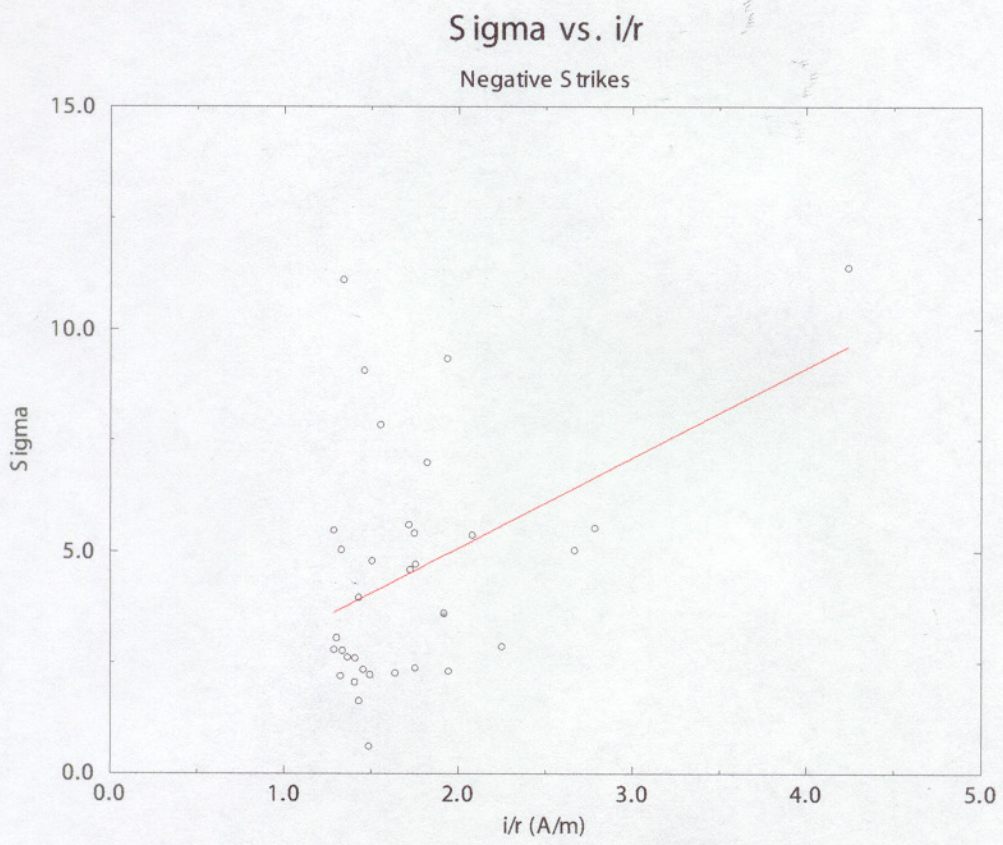
Sigma vs. i/r
Negative Strikes
15.0
10.0
5.0
0.0
Sigma
0.0
1.0
2.0
3.0
4.0
5.0
i/r (A/m)

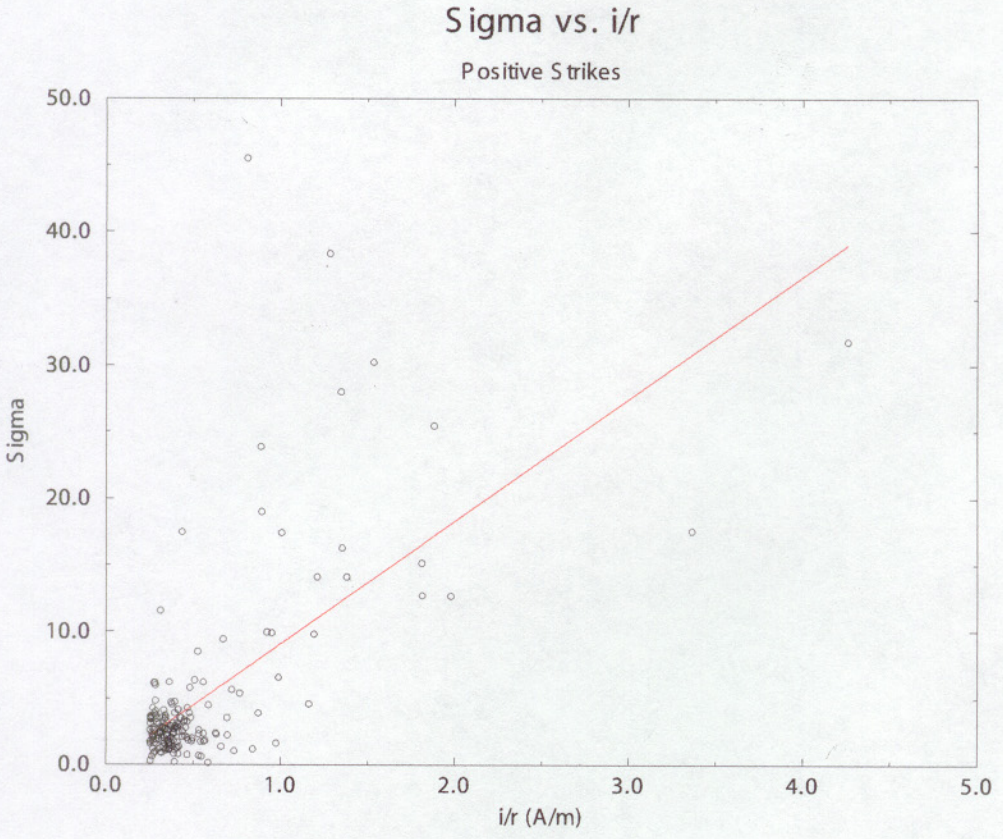
Sigma vs. i/r
Positive Strikes
50.0
40.0
30.0
20.0
10.0
0.0
Sigma
0.0
1.0
2.0
3.0
4.0
5.0
i/r (A/m)

Negative

Table 1

All Strikes			X	Y	Z	Σ
i/r (kA/km)	Peak Current (kA)	Distance (km)	Δ Signal	Δ Signal	Δ Signal	Δ Signal
4.24	118.8	28.02	2200	2500	2500	4164
2.78	68.7	24.69	1100	2000	1900	2970
2.67	90.8	34.04	600	1500	1800	2419
2.25	72	32.01	500	700	900	1245
2.08	70	33.65	500	800	950	1339
1.94	60.3	31.05	600	600	800	1166
1.94	105.1	54.31	1400	1100	1250	2175
1.92	109.2	56.99	1600	900	1100	2140
1.75	45.6	26.12	800	800	750	1357
1.72	92.1	53.47	1100	700	700	1480
1.71	45.9	26.78	1400	2250	2600	3712
1.71	45.9	26.79	1100	2400	2900	3922
1.55	90.5	58.38	450	300	600	808
1.49	42.3	28.35		900	900	1273
1.49	46.2	31.11	400	800	900	1269
1.45	40.5	27.87		1700	900	1924
1.40	66.1	47.11	400	200	350	568
1.33	85.4	64.41	1100	350	600	1301
1.24	35.4	28.52		400	500	640
1.23	33	26.8		1000	1100	1487
1.19	68.9	57.72	0	400	600	721
1.19	64.6	54.5	500	300	500	768
1.18	70.5	59.82	600	500	0	781
1.15	68.7	59.58	600	700	250	955
1.12	61	54.56	600	0	500	781
1.11	29	26.04		600	800	1082
1.11	28.9	26.1		450	1600	570
1.09	29.6	27.06		800	700	1063
1.08	69.9	64.6998	1100	600	600	1389
1.04	68.3	65.533	400	200	700	831
0.97	70.9	73.1076	600	600	500	985
0.95	26.4	27.86		600	500	781
0.94	49.7	52.78	600	500	550	955
0.92	47.8	51.72	800	500	750	1205
0.88	90	102.46	200	200	400	490
0.87	47.8	55.05	400	250	200	512
0.87	24.1	27.82		700	400	806
0.84	46.4	55.47	400	250	200	512
0.83	49.9	60.22	1100	700	750	1504
0.81	50	61.38	400		300	500
0.80	21.3	26.46		500	300	707
0.80	46.8	58.49	600	450	500	901
0.79	46.8	59.32	500	250	400	687
0.75	46.2	61.94		400	550	680

Positive

Negative

Signal vs. Distance

Table 2

Peak Current ~ 48 kA		X	Y	Z	Σ
Distance (km)	Peak Current (kA)	Δ Signal	Δ Signal	Δ Signal	Δ Signal
26.79	45.9	1100	2400	2900	3922
28.55	50	40	700	900	1141
31.11	46.2	400	800	900	1269
51.72	47.8	800	500	750	1205
52.78	49.7	600	500	550	955
55.05	47.8	400	250	200	512
55.47	46.4	400	250	200	512
58.49	46.8	600	450	500	901
59.32	46.8	500	250	400	687
60.22	49.9	1100	700	750	1504
61.38	50	400		300	500
61.94	46.2		400	550	680

Table 3

Peak Current ~ 91 kA		X	Y	Z	Σ
Distance (km)	Peak Current (kA)	Δ Signal	Δ Signal	Δ Signal	Δ Signal
34.04	90.8	600	1500	1800	2419
53.47	92.1	1100	700	700	1480
58.38	90.5	450	300	600	808
102.46	90	200	200	400	490

Signal vs. Peak Current

Table 4

Distance ~ 28 km		X	Y	Z	Σ
Peak Current (kA)	Distance (km)	Δ Signal	Δ Signal	Δ Signal	Δ Signal
118.8	28.02	2200	2500	2500	4164
50	28.55		600	700	922
45.9	26.78	1400	2250	2600	3712
42.3	28.35		900	900	1273
40.5	27.87		1700	900	1924
35.4	28.52		400	500	640
33	26.8		1000	1100	1487
29.6	27.06		800	700	1063
26.4	27.86		600	500	781
24.1	27.82		700	400	806

Table 5

Distance ~ 25.5 km		X	Y	Z	Σ
Strength (kA)	Distance (km)	Δ Signal	Δ Signal	Δ Signal	Δ Signal
68.7	24.69	1100	2000	1900	2454
45.6	26.12	800	800	750	2042
29	26.04		600	800	721
28.9	26.1		450	1600	1097
21.3	26.46		500	300	943

Positive

Table 6

All Strikes			X	Y	Z	Σ
i/r (kA/km)	Peak Current (kA)	Distance (km)	Δ Signal	Δ Signal	Δ Signal	Δ Signal
6.48	129.1	19.91	12500	10000	17000	23351
4.26	95.1	22.33	6500	4800	6000	10064
3.37	90.3	26.82	3100	2250	3100	4928
1.81	150.3	82.828	2100	1100	1500	2805
1.80	37.1	20.65	1800	1000	1600	2608
1.54	131	85.29	2600	600	1350	2990
1.35	86.3	63.72	2400	500	1100	2687
1.28	33	25.71	1800	1600	2600	3544
1.16	30.3	26.05	1500	1500	900	2304
0.99	141.8	143.33	1600	800	900	2002
0.95	82	86.37	1300	950	1200	2008
0.92	87	94.37	1200	800	800	1649
0.89	20.5	23.0239	1000	400	950	1436
0.87	61.1	69.83	600	2600	900	2816
0.87	78.1	89.35	400	900	300	1030
0.81	71.6	88.46	1500	500	900	1819
0.72	101.5	140.59	1200	500	1100	1703
0.63	132.5	209.167	0	600	1000	1166
0.58	100	170.95	800	300	200	877
0.56	83.8	149.78	0	400	400	566
0.56	81.8	146.8	1400	600	400	1575
0.53	145.9	273.55	200	400	100	458
0.42	86.1	205.85	400	500	400	755
0.41	90.5	218.98	0	600	500	781
0.41	86.3	210.995	0	700	500	860
0.39	86.8	220.09	0	400	550	680
0.39	114.5	290.68	400	600	600	938

Signal vs. Distance

Table 7

Peak Current ~ 87 kA		X	Y	Z	Σ
Distance (km)	Peak Current (kA)	Δ Signal	Δ Signal	Δ Signal	Δ Signal
26.82	90.3	3100	2250	3100	4928
63.72	86.3	2400	500	1100	2687
94.37	87	1200	800	800	1649
205.85	86.1	400	500	400	755
210.995	86.3	0	700	500	860
218.98	90.5	0	600	500	781
220.09	86.8	0	400	550	680

Signal vs. Peak Current

Table 8

Distance ~ 21 km		X	Y	Z	Σ
Peak Current (kA)	Distance (km)	Δ Signal	Δ Signal	Δ Signal	Δ Signal
129.1	19.91	12500	10000	17000	23351
95.1	22.33	6500	4800	6000	10064
37.1	20.65	1800	1000	1600	2608

Table 9

Distance ~ 87.5 km		X	Y	Z	Σ
Peak Current (kA)	Distance (km)	Δ Signal	Δ Signal	Δ Signal	Δ Signal
150.3	82.82	2100	1100	1500	2805
131	85.29	2600	600	1350	2990
82	86.37	1300	950	1200	2008
71.6	88.46	1500	600	1450	1819

Table 10

		m	±	ln(a)	±	Cor
Negative	~48 kA	-1.3	0.5	12	2	0.65
Distance	~91 kA	-1.5	0.3	13	1.3	0.96
	Combined	-1.3	0.3			
Peak Current	~28 km	1	1	3	4	0.33
	~25.5 km	1.0	0.14	3.6	1.1	0.88
	Combined	1.0	0.5			
i/r		1.0	0.14	6.76	0.07	0.73
Positive						
Distance	~87 kA	-0.92	0.05	11.6	0.2	0.99
Peak Current	~21 km	1.7	0.3	1.7	1.1	0.99
	~87.5 km	0.7	0.13	4.7	0.6	0.96
	Combined	1.2	0.2			
i/r		1.1	0.1	7.5	0.06	0.93

Table 11

	Frequency	Cut Point	m	±	b	±	Cor	i/r
Negative	~~80-100~~	~~0.75~~	~~2.5~~	~~1.5~~	~~4.2~~	~~1.8~~	~~0.13~~	~~0.32~~
	~~140-160~~	~~0.5~~	~~0.9~~	~~0.3~~	~~2.1~~	~~0.2~~	~~0.15~~	~~3.2~~
	205-215	0.9	2.5	0.5	-0.2	0.7	0.43	2.1
	265-275	0.6	2	0.3	0.7	0.3	0.36	2.2
	~~325-335~~	~~0.5~~	~~0.16~~	~~0.15~~	~~2.37~~	~~0.13~~	~~0.05~~	~~16.4~~
	~~385-395~~	~~0.22~~	~~0.74~~	~~0.09~~	~~1.49~~	~~0.04~~	~~0.2~~	~~4.7~~
	~~445-455~~	~~1.1~~	~~1.2~~	~~0.4~~	~~0.5~~	~~0.6~~	~~0.43~~	~~3.8~~
	505-515	0.7	2.3	0.3	0	0.4	0.44	2.2
	All	1.25	2	0.8	1	1.4	0.44	1.97
Positive	~~80-100~~	~~0.1~~	~~28.2~~	~~1.1~~	~~-0.4~~	~~0.4~~	~~0.66~~	~~0.19~~
	~~140-160~~	~~0.1~~	~~13~~	~~0.6~~	~~0.4~~	~~0.2~~	~~0.61~~	~~0.35~~
	205-215	0.3	3.9	0.5	0.8	0.4	0.59	1.1
	265-275	0.2	1.8	0.4	1.5	0.2	0.3	1.9
	~~325-335~~	~~0.35~~	~~1~~	~~0.3~~	~~2~~	~~0.3~~	~~0.33~~	~~3~~
	~~385-395~~	~~0.3~~	~~1.7~~	~~0.3~~	~~1.2~~	~~0.2~~	~~0.46~~	~~2.2~~
	~~445-455~~	~~0.2~~	~~0.46~~	~~0.17~~	~~2.3~~	~~0.1~~	~~0.17~~	~~5.9~~
	505-515	0.25	3	0.4	0.8	0.3	0.47	1.4
	All	0.25	9.2	0.8	-0.1	0.6	0.66	0.55

Table 12

Frequency	# Mag	# File	# Cor	%Mag (Ncor/Nmag)	%File (Ncor/Nfile)
205-215	6459	19	12	0.19%	63%
265-275	761	8	2	0.26%	25%
505-515	181	12	4	2.21%	33%
All	6783	45	27	0.40%	60%